Taylor & Francis
Taylor & Francis Group

BRIEF REPORT

&#8203; OPEN ACCESS   Check for updates

# Detection of neoantigen-specific T cells following a personalized vaccine in a patient with glioblastoma

Tanner M. Johanns[a,b], Christopher A. Miller[c], Connor J. Liu[b,d], Richard J. Perrin[e], Diane Bender[b], Dale K. Kobayashi[b], Jian L. Campian[a], Michael R. Chicoine[d], Ralph G. Dacey[d], Jiayi Huang[f], Edward F. Fritsch[g], William E. Gillanders[b,h], Maxim N. Artyomov[b,e], Elaine R. Mardis[i], Robert D. Schreiber[b,e], and Gavin P. Dunn[b,d]

[a]Division of Medical Oncology, Washington University School of Medicine, St. Louis, MO, USA; [b]Andrew M. and Jane M. Bursky Center for Human Immunology and Immunotherapy Programs, Washington University School of Medicine, St. Louis, MO, USA; [c]The McDonnell Genome Institute, Washington University in St. Louis, St. Louis, MO, USA; [d]Department of Neurological Surgery, Washington University School of Medicine, St. Louis, MO, USA; [e]Department of Pathology and Immunology, Washington University School of Medicine, St. Louis, MO, USA; [f]Department of Radiation Oncology, Washington University in St. Louis, St. Louis, MO, USA; [g]Neon Therapeutics, Cambridge, MA, USA; [h]Department of Surgery, Section of Endocrine and Oncologic Surgery, Washington University School of Medicine, St. Louis, MO, USA; [i]Institute for Genomic Medicine, Nationwide Children's Hospital and The Ohio State University, Columbus, OH, USA

## ABSTRACT

Neoantigens represent promising targets for personalized cancer vaccine strategies. However, the feasibility of this approach in lower mutational burden tumors like glioblastoma (GBM) remains unknown. We have previously reported the use of an immunogenomics pipeline to identify candidate neoantigens in preclinical models of GBM. Here, we report the application of the same immunogenomics pipeline to identify candidate neoantigens and guide screening for neoantigen-specific T cell responses in a patient with GBM treated with a personalized synthetic long peptide vaccine following autologous tumor lysate DC vaccination. Following vaccination, reactivity to three HLA class I- and five HLA class II-restricted candidate neoantigens were detected by IFN-γ ELISPOT in peripheral blood. A similar pattern of reactivity was observed among isolated post-treatment tumor-infiltrating lymphocytes. Genomic analysis of pre- and post-treatment GBM reflected clonal remodeling. These data demonstrate the feasibility and translational potential of a therapeutic neoantigen-based vaccine approach in patients with primary CNS tumors.

## Introduction

Cancer immunogenomics incorporates next-generation sequencing and bioinformatics to predict which tumor-specific somatic alterations may produce candidate neoantigens that could bind with high affinity to host MHC molecules and potentially be recognized by the anti-tumor immune response.[1] Due to their tumor-restricted expression, neoantigens represent compelling targets for personalized cancer vaccines.[2–7] In preclinical tumor models, polyvalent neoantigen vaccines can be therapeutically effective.[8,9] Furthermore, neoantigen-based vaccines can elicit immune responses in patients,[2,6,7] although these studies have been restricted to melanoma, which generally possesses high mutational burdens, and therefore, potentially contains a high number of candidate neoantigens. Thus, it remains unclear whether targeting neoantigens is feasible in cancers with lower mutational burdens.

We have previously reported the successful use of an immunogenomics pipeline to identify candidate neoantigens in two preclinical mouse models of glioblastoma.[10] We used IFN-γ ELISPOT and neoantigen-specific tetramer assays to identify the presence of neoantigen-specific T cell responses in two orthotopic transplantable models. These data support the hypothesis that CNS immunosurveillance is operational and capable of inducing an endogenous neoantigen-specific T cell response against intracranial tumors. However, given that these preclinical models harbor a carcinogen-induced high mutational burden not typically seen in patients with glioblastoma, it is unclear if a similar immunogenomics-based neoantigen discovery platform will translate clinically. Notably, a recent report demonstrated the generation of neoantigen-specific T cell responses following an autologous tumor lysate-dendritic cell vaccine in patients with ovarian carcinoma, a tumor with comparable tumor mutational load as glioblastoma.[11,12]

Here, we report a patient with glioblastoma (GBM) treated with a heterologous personalized vaccine, including an autologous tumor lysate-dendritic cell vaccine (DCVax) followed by a neoantigen-based synthetic long peptide vaccine (GBM.PVax). Analysis of post-treatment peripheral blood demonstrated detectable neoantigen-specific CD8^{+} and CD4^{+} T cell responses after peptide vaccination. Similar responses were observed in post-treatment tumor-infiltrating lymphocytes (TIL). Furthermore, genomic and transcriptomic characterization of the mutational

Color versions of one or more of the figures in the article can be found online at www.tandfonline.com/koni.
&#9401; Supplemental data for this article can be accessed on the publisher's website.

landscape and tumor microenvironment pre- and post-treatment demonstrated tumor clonal evolution and evidence of potential immune evasion. Together, these results support the evaluation of immunogenomics-based vaccine strategies in glioblastoma and other tumors exhibiting moderate mutational loads.

## Results

### Case report

A 66-year-old previously healthy female presented with new-onset seizures, and a diagnostic brain MRI revealed a right parietal contrast-enhancing lesion. A near gross total resection was performed (>99% extent), and pathology revealed GBM with an unmethylated $O^6$-methylguanine-DNA methyltransferase (MGMT) promoter, presence of mutated TERT promoter (C228T), and absence of IDH1/2 mutations – molecular features associated with chemotherapy resistance and decreased overall survival.[13-15]

Prior to surgery, the patient had consented to an autologous tumor lysate-dendritic cell vaccine study (DCVax-L) (NCT00045968) and an institutional personalized neoantigen-based peptide vaccine study (GBM.PVax) (NCT02510950). Therefore, following 6 weeks of standard adjuvant radiation therapy and concurrent temozolomide chemotherapy (CCRT), the patient received DCVax-L plus temozolomide during GBM.PVax preparation (Figure 1). DCVax-L was administered off-trial due to radiographic pseudoprogression noted following CCRT (data not shown). After cycle 4 of DCVax-L, GBM.PVax manufacturing was complete so DCVax-L was discontinued and GBM.PVax was initiated.

To design GBM.PVax, DNA whole exome sequencing of the resected tumor revealed 52 somatic, missense mutations (Figure 2(a), Supplementary File). High-affinity ($ic_{50}$ <500 nM) candidate neoantigens were identified using the neoantigen discovery pipeline, pVAC-Seq, as well as the NetMHCIIpan 3.2 and NetMHCII 2.3 algorithms,[10,16] revealing 2 HLA class I-restricted candidates, 32 HLA class II-restricted candidates, and 14 candidates with high affinity to both HLA class I and II alleles (Figure 2(a)). Eight synthetic long peptides (SLPs) encompassing seven neoantigens were successfully synthesized for inclusion into GBM.PVax (Figure 2(b)).

After cycle 1 of GBM.PVax, the patient developed confusion, and a brain MRI revealed increased T2/FLAIR indicative of edema/inflammation along with increased size of the T1 contrast-enhancing lesion most consistent with pseudoprogression (Figure 2(c)). Symptoms resolved completely with

a short steroid taper, and a repeat brain MRI 4 weeks later showed a reduction in T2/FLAIR with stabilization of the T1 contrast-enhancing lesion (Figure 2(c)) coinciding with a significantly improved functional status. The patient continued to do well clinically through cycles 3 and 4 of GBM. PVax and noted interval development of axillary lymphadenopathy. Unfortunately, the subsequent brain MRI was concerning for disease progression (Figure 2(c)), and a repeat craniotomy with subtotal resection was performed. Histopathology demonstrated extensive treatment effect with only focal areas of residual glioma, and no overt tumor recurrence indicating the changes on the MRI was again due to pseudoprogression (Figure 2(d)). The post-surgical course was complicated by a saddle pulmonary embolus treated with embolectomy; intraparenchymal hemorrhage plus gastrointestinal bleeding from anticoagulation therapy resulting in a declining functional status that precluded additional GBM-related therapy. The patient passed away 21 months after initial diagnosis (Figure 1).

### Immunogenicity of personalized vaccine

To assess for the presence of neoantigen-specific T cells post-vaccination, we first evaluated the immunogenicity of the known peptides contained within GBM.PVax as the antigens present in DCVax-L were undefined. First, reactivity to the predicted immunodominant minimal epitopes of the GBM.PVax peptides (Table 1) was determined in PBMC obtained 4 months after initiation of GBM.PVax using IFN-γ ELISPOT. Isolated post-vaccination CD8$^+$ T cells reacted to the HLA-B*44:02-restricted neoantigen, GPR133$_{G126E}$ (mGPR133), while CD4$^+$ T cells were reactive to both IL22$_{V72I}$ (mIL22) and PTEN$_{R47S}$ (mPTEN) (Figure 3(a)). An expanded screen of alternative mutation-containing minimal epitopes did not reveal additional reactivity to any of the GBM.PVax-containing neoantigens (data not shown). Reactivity to mGPR133, mIL22, and mPTEN appeared to be mutation-specific as no T cell reactivity was observed to the corresponding wild-type epitopes (Figure 3(b)). In order to determine whether these neoantigen-specific responses were induced or augmented by vaccination rather than as a result of prior therapies, reactivity was also measured in a PBMC sample obtained immediately prior to GBM.PVax but after the completion of DCVax-L administration. A pre-existing CD8$^+$ T cell response to mGPR133 was present above background prior to GBM.PVax but increased after peptide vaccination (Figure 3(c)). As a control for normal variation over time, CD8$^+$ T cell reactivity to HLA-A*24:02 and B*44:02-restricted CMV antigens was observed prior to GBM.PVax and was noted to decrease between
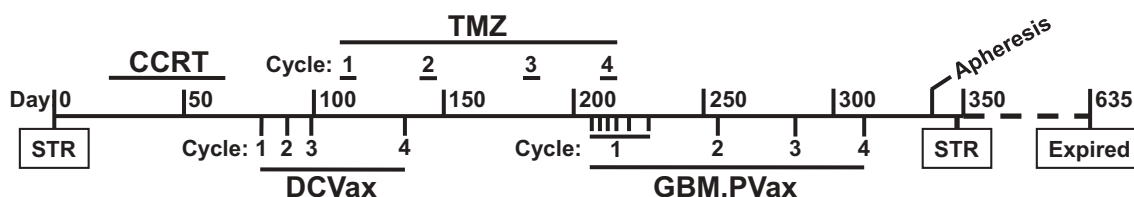


**Figure 1.** Schematic representation of treatment course. Note: cycle 3 of temozolomide was delayed due to thrombocytopenia, and cycle 4 was given at a reduced dose (100 mg/m$^2$ down from 150 mg/m$^2$) due to intolerance. Abbreviations: STR = subtotal resection; CCRT = concurrent chemoradiation therapy; TMZ = temozolomide; DCVax = autologous tumor lysate-dendritic cell vaccine.
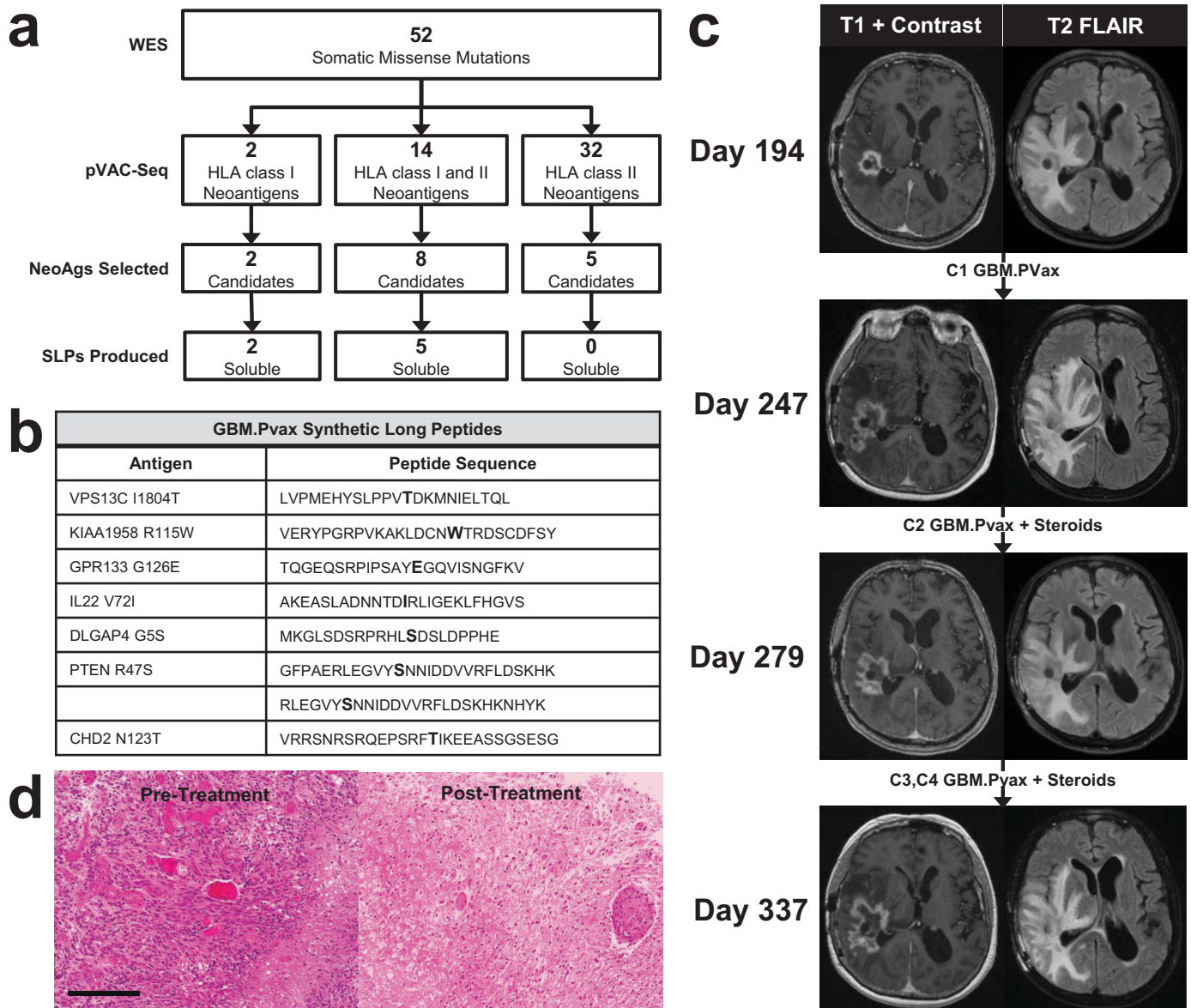
**Figure 2.** Design and response of a personalized neoantigen-based peptide vaccine for a patient with glioblastoma. (a) Schematic diagram of GBM.PVax design. Non-synonymous missense mutations are identified by comparing patient-matched PBMC (normal) and tumor DNA whole exome sequencing, then mutations are filtered through *in silico* neoantigen discovery pipelines to identify high-affinity HLA class I and/or class II candidates. Top candidates were selected for peptide synthesis as long peptides (SLPs). Soluble SLPs are incorporated into GBM.PVax. (b) Table listing the 8 SLPs encompassing 7 neoantigens included in GBM.PVax. The location of the mutated amino acid is enlarged and bolded. (c) Representative brain MRI axial images at indicated time points during treatment with GBM.PVax. (d) Representative H&E sections from initial tumor resection (day 0) and post-treatment tumor resection (day 347). Black line denotes 200 microns.

the pre- and post-GBM.PVax time points (Figure 3(c)), suggesting that mGPR133 reactivity was likely boosted as a result of GBM.PVax immunization. Neither mIL22-specific nor mPTEN-specific CD4$^+$ T cell responses were detectable above background prior to GBM.PVax initiation, suggesting both were increased to detectable levels after immunization with GBM.PVax (Figure 3(c)).

Because immunity to neoantigens could also develop secondary to prior therapies (i.e. surgery, radiation, temozolomide and/or DCVax-L) or epitope spreading following peptide vaccination, we evaluated reactivity to predicted high-affinity neoantigen candidates not targeted by GBM.PVax (Table 1). Interestingly, lower level CD8$^+$ T cell responses were observed to PDIA3$_{T219S}$ (mPDIA3) and WDR63$_{T690M}$

(mWDR63), while CD4$^+$ T cell reactivity was noted to MEGF8$_{P238S}$ (mMEGF8), NUP107$_{R558H}$ (mNUP107), and NVL$_{I644V}$ (mNVL) in post-vaccination PBMC (Figure 3(d)). Due to lack of additional pre-GBM.PVax PBMC availability, further characterization of the induction and kinetics of these additional neoantigen-specific immune responses was not possible.

### Presence of neoantigen-specific TIL following treatment

Next, the presence of neoantigen-specific responses in TIL isolated from the second surgical specimen was assessed. Consistent with PBMC, reactivity to mGPR133, mWDR63, mIL22, mPTEN, and mNVL was observed above background among CD8$^+$ or CD4$^+$ TIL, however, only responses to

Table 1. Table of minimal epitope sequences of HLA class I and II-restricted GBM.PVax and non-GBM.PVax neoantigens screened by IFN-γ ELISPOT for T cell reactivity including corresponding predicted binding affinity (ic$_{50}$). The location of the mutated amino acid is enlarged and underlined.

| Neoantigen | core sequence | Iv50 (nM) | GBM.PVax |
|---|---|---|---|
| **HLA-A*01:01** | | | |
| KIAA1958 R115W | **W**TRDSCDFSY | 368 | Yes |
| **HLA-A*24:02** | | | |
| ZMYND12 R192H | **H**YHLANDIYF | 171 | No |
| **HLA-B*44:02** | | | |
| GPR133 G126E | YEGQVISNGF | 260 | Yes |
| **HLA-C*05:01** | | | |
| VPS13C I1804T | VTDKMNIEL | 55 | Yes |
| PTEN R47S | YSNNIDDVV | 112 | Yes |
| IL22 V72I | LADNNTDIR | 138 | Yes |
| DLGAP4 G5S | LSDSRPRHL | 239 | Yes |
| PDIA3 T219S | FEDKSVAYT | 380 | No |
| MEGF8 P238S | LSSPGLLAV | 383 | No |
| **HLA-C*06:02** | | | |
| WDR3 T690M | FYNDIILMV | 109 | No |
| CHD2 N123T | SRQEPSRFT | 230 | Yes |
| **HLA-DRB*01:01** | | | |
| MEGF8 P238S | AGAFLSSPGLLAVFG | 5 | No |
| SIRPB1 T18M | LLMMLLLGRLTGVAG | 8 | No |
| NVL I644V | GLNFVSVKGPELLNM | 9 | No |
| NUP107 R558H | LILFFHTLGLQTKEE | 10 | No |
| IL22 V72I | NNTDIRLIGEKLFHG | 51 | Yes |
| PTEN R47S | GFPAERLEGVYSNNI | 192 | Yes |
| VPS13C I1804T | PMEHYSLPPVTDKMN | 196 | Yes |
| GPR133 G126E | PSAYEGQVISNGFV | 282 | Yes |
| CHD2 N123T | SNRSRQEPSRFTIKE | 325 | Yes |

mGPR133, mIL22, and mNVL were significant (Figure 4(a)). Spatially, immunohistochemistry demonstrated that T cells were predominantly restricted to the perivascular space, though infiltration into the pauci-cellular intraparenchymal region was also observed (Figure 4(b)).

### Treatment-related clonal evolution following treatment

To explore the effect of treatment on tumor evolution, the mutational landscape and clonal architecture of the pre- and post-treatment tumor specimens were characterized by whole exome DNA sequencing. SciClone analysis revealed loss of two pre-treatment subclonal populations (clusters 2 and 4) but emergence of two additional sub-populations (clusters 3 and 5) post-treatment (Figure 4(c)). T cell reactivity was observed to neoantigens both private to the lost pre-treatment subclones (mGPR133, mMEGF8, and mNUP107) and shared within the founder clone (mWDR63, mPDIA3, mIL22, mPTEN, and mNVL) (Figure 4(c)). Although transcriptional repression of neoantigens has been suggested to facilitate immune escape,[17,18] no changes were observed in transcriptional expression levels among the founder clone neoantigens between pre- and post-treatment specimens (Supplementary File). Furthermore, there was no observed
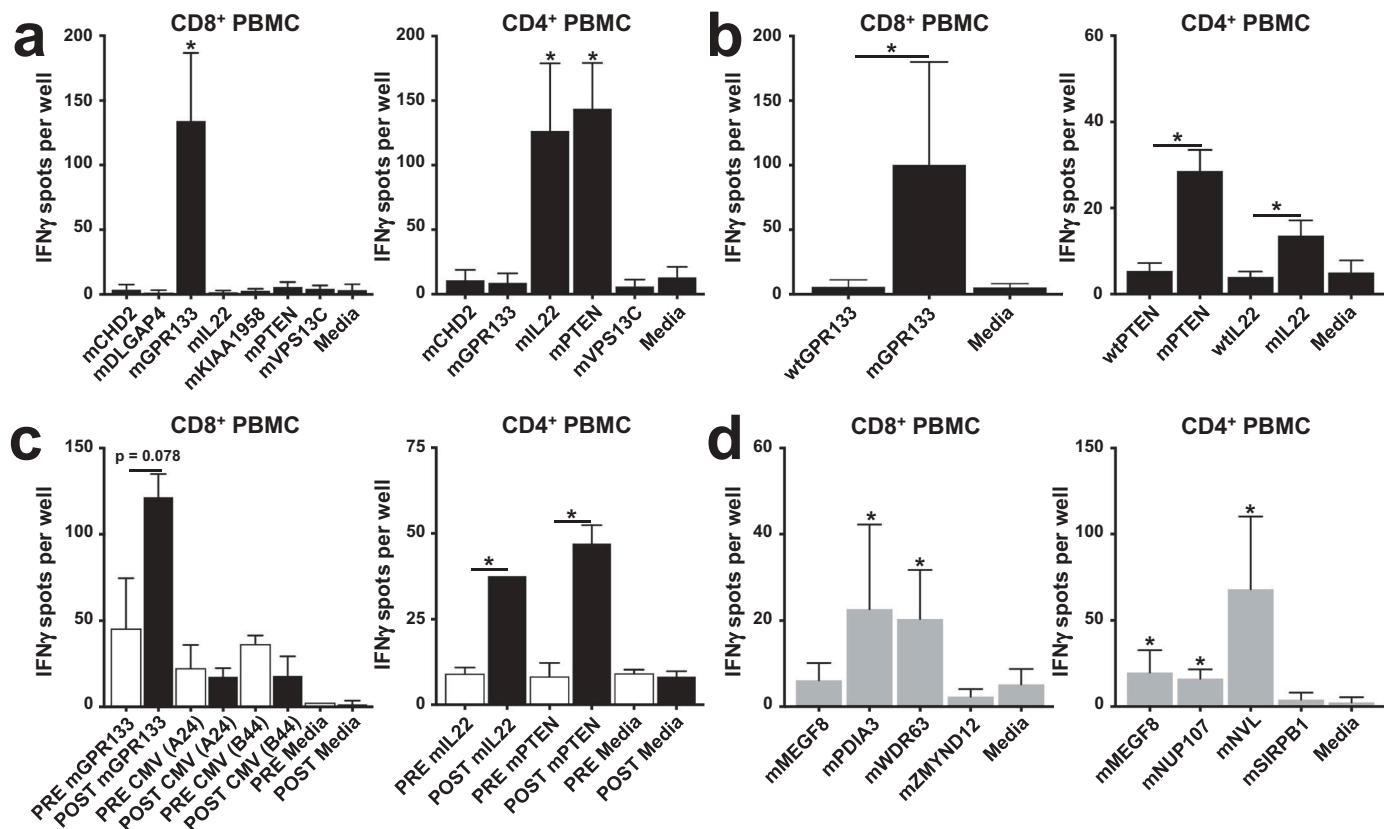
**Figure 3.** Immunogenicity of GBM.PVax in peripheral blood. (a-d) Bar graphs from IFN-γ ELISPOT data of positively selected CD8^{+} (left column) and CD4^{+} (right column) PBMC stimulated with indicated peptide. Media = negative control (no peptide). (a) Reactivity screen to GBM.PVax neoantigens. (b) Comparison of reactivity between mutated and wild-type GBM.PVax neoantigens that demonstrated positive reactivity in Figure 3(a). (c) Comparison of reactivity between pre- and post-GBM.PVax PBMC. (d) Reactivity screen of non-GBM.PVax neoantigens from Table 1. A, b, and d represent a minimum of two independent experiments done in duplicate. (c) represents a single experiment done in duplicate due to limited sample. (*) represents p < 0.05 compared to negative control unless otherwise indicated.
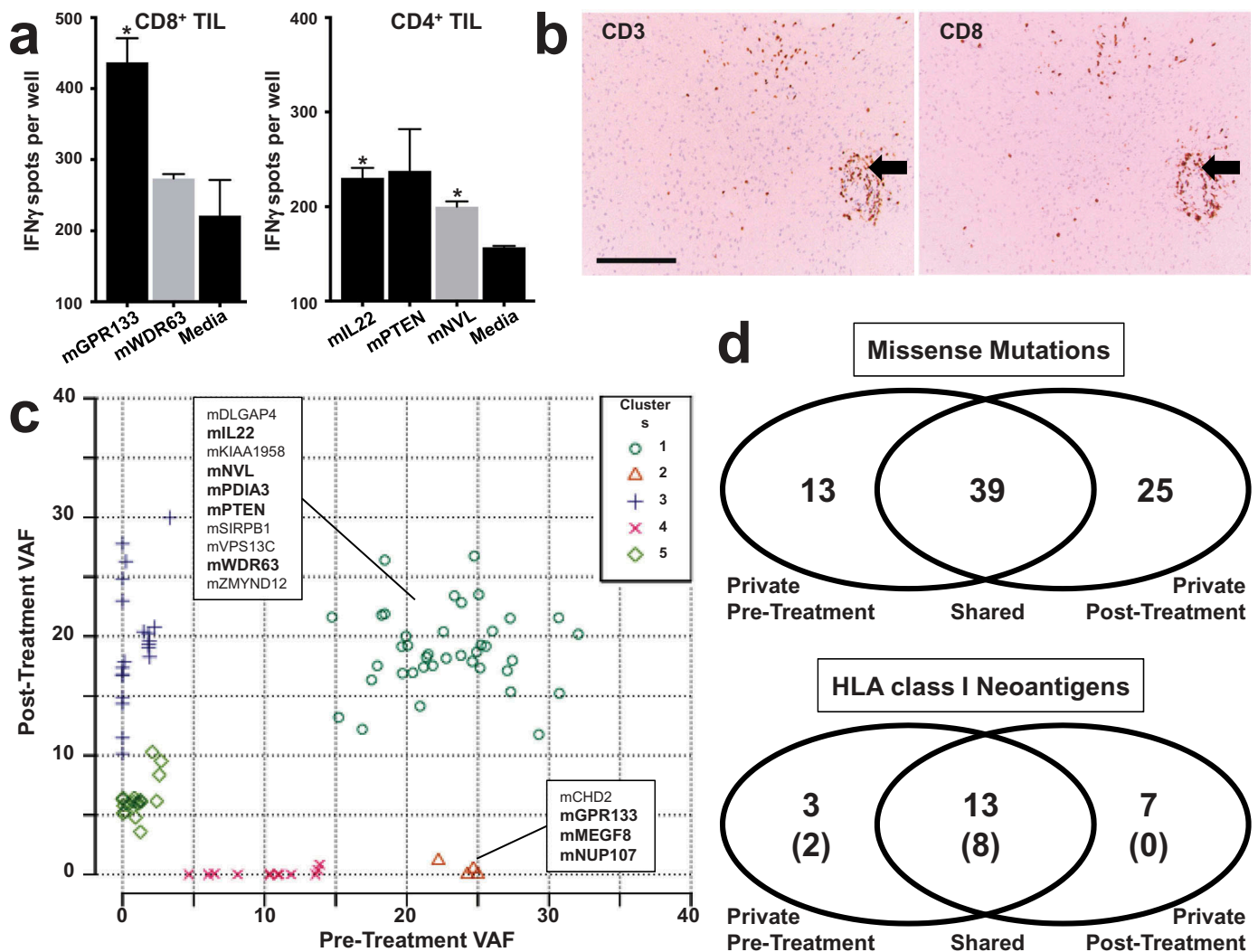
**Figure 4.** Clonal evolution of neoantigens after treatment. (a) Bar graphs from IFN-γ ELISPOT data of positively selected CD8^{+} (left column) and CD4^{+} (right column) *ex vivo* expanded TIL isolated from the post-GBM.PVax specimen and stimulated with indicated peptide. Media = negative control (no peptide). Graphs represent a single experiment done in duplicate due to limited sample. (*) represents p < 0.05 compared to negative control. (b) Representative immunohistochemistry sections of anti-CD3 and anti-CD8 staining in the post-treatment resection specimen. Black arrow identifies perivascular lymphocytes. Black line denotes 200 microns. (c) SciClone plot of clonal and subclonal populations present in pre- and post-treatment tumor specimens. VAF = variant allele fraction. Cluster 1 = founder clone mutations. Bolded neoantigens represent those with observed reactivity by ELISPOT. (d) Venn diagrams of missense mutations (left) and predicted high-affinity HLA class I neoantigens (right) from the pre- and post-treatment tumor specimens. Numbers indicate respective private or shared missense mutations or neoantigens. Parentheses represent the number of neoantigens with confirmed expression by RNA-seq.

transcriptional repression or loss of heterozygosity of HLA loci (Supplementary File and data not shown).

In the post-treatment tumor, 7 of the 25 private mutations were predicted to generate at least one high-affinity HLA class I-restricted neoantigen, a similar frequency (28%) to the shared founder clone (33.3%) and private pre-treatment subclones (23%) (Figure 4(d)) suggesting equivalent somatic mutation and neoantigen rates within the sub-populations. However, while RNA expression was detected for 2 of 3 and 8 of 13 neoantigens in the private pre-treatment subclones and founder clone, respectively, no private post-treatment neoantigen RNA expression was detectable (Figure 4(d) and Supplementary File), suggestive of possible immunoediting.

### Immunologic evolution during treatment

To characterize the effects of treatment on the broader immune microenvironment, we compared pre- and post-

treatment transcriptomes. Analyses revealed increased relative expression levels for genes associated with both T cell (*CD4, CD8A*) subsets (Figure 5(a)). An increase in cytotoxic CD8 T cell effector function genes (*PRF1, GZMA, GZMB*) was also noted to be upregulated (Figure 5(a)). Among the CD4 T helper lineage, increased expression of the Treg, Th2 and Th17 lineage-defining transcription factors *FOXP3, GATA3*, and *RORC*, respectively, were upregulated post-treatment, while the Th1 master regulator transcription factor, T-bet (*TBX21*), was downregulated (Figure 5(a)). Consistent with the decreased expression of *TBX21* and increased expression of *FOXP3, IFNG* was not found to be expressed in the post-treatment specimen (data not shown), while *IL10* was noted to be upregulated (Figure 5(a)), respectively. Similarly, several isoforms of the Th17 effector cytokine, IL-17, were upregulated (*IL17B* and *IL17D*) though other isoforms (*IL17A, IL17C, IL17E, IL17F*) were not detected (Figure 5(a)) and
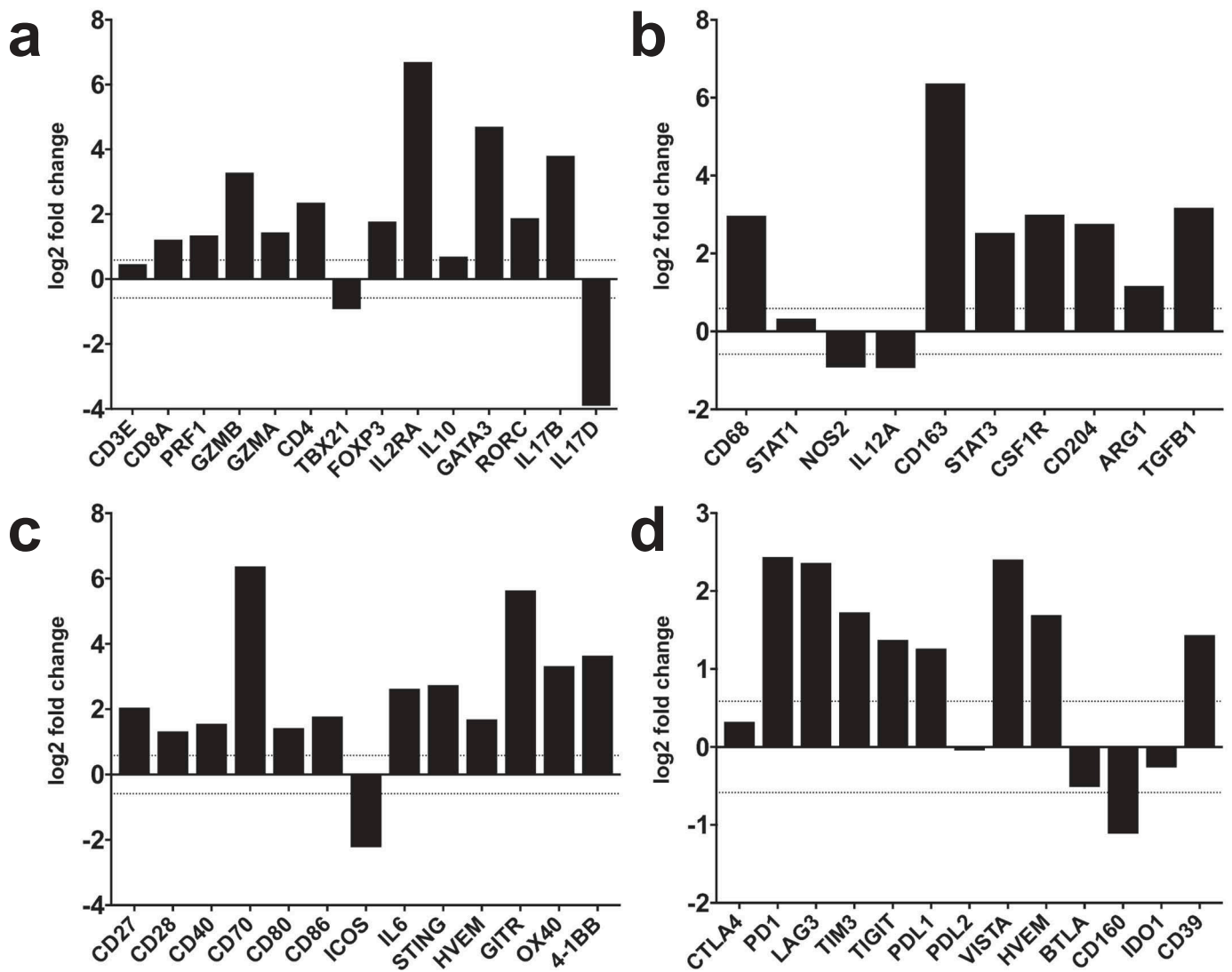
**Figure 5.** Immune landscape of the pre- and post-treatment tumor microenvironment. (a-d) Bar graphs demonstrate the relative gene expression level (log2 fold change) of indicated immune cell subsets (a, b) or immune checkpoint molecules (c, d) derived from bulk RNA-seq. Dotted line indicates +1.5 and −1.5 log2 fold changes.

data not shown). Expression of the Th2 effector cytokine, IL-4 (*IL4*) was also not detected in either the pre- or post-treatment specimens (data not shown). Together, these data demonstrate that treatment with radiation, chemotherapy, and vaccination resulted in an overall increase in the relative gene expression profile of cytotoxic CD8 T cells and non-Th1 CD4 T cell subsets, including regulatory T cells, within the tumor microenvironment.

A similar mixed response was seen among the myeloid compartment following treatment with a noted increase in relative expression levels of both M1 (*CD68, STAT1*) and M2 (*CD163, STAT3*) macrophages/microglia compared to pre-treatment,[19] (Figure 5(b)). However, there appeared to be an overall skewing toward a predominant M2 environment with the noted upregulation of M2-associated genes *CSF1R, CD206, ARG1,* and *TGFB1*, whereas M1-associated genes *NOS2* and *IL12A* were relatively downregulated. Consistently, a similar increase of M2 macrophages has been reported in GBM patients treated with DCVax following standard chemoradiation.[20]

Next, we compared expression patterns of select co-stimulatory and co-inhibitory immune checkpoint molecules. Genes associated with the co-stimulatory molecules OX40 4–1BB, CD27, and CD70, as well as the co-inhibitory molecules PD-1, PD-L1, TIM-3, GITR, VISTA, TIGIT, and LAG3 were broadly upregulated (Figure 5(c)). Of note, other clinically actionable immune checkpoint targets (i.e. CTLA4, IDO1, ICOS, and PDL2) were unchanged or downregulated after treatment (Figure 5(c)) suggesting there was not a global upregulation of these molecules between specimens.

To provide an integrated overview of treatment-related changes in the immune landscape, we applied a previously described gene set enrichment analysis (GSEA) approach[21] in which non-overlapping metagene sets corresponding to functional immune modules – antigen processing/presentation (MHC), checkpoints (CP), effector cells (EC), and suppressor cells (SC) – were normalized to 166 TCGA GBM samples. We then compared GSEA analysis of transcriptomic data before and after treatment to this reference dataset (Figure 6). This
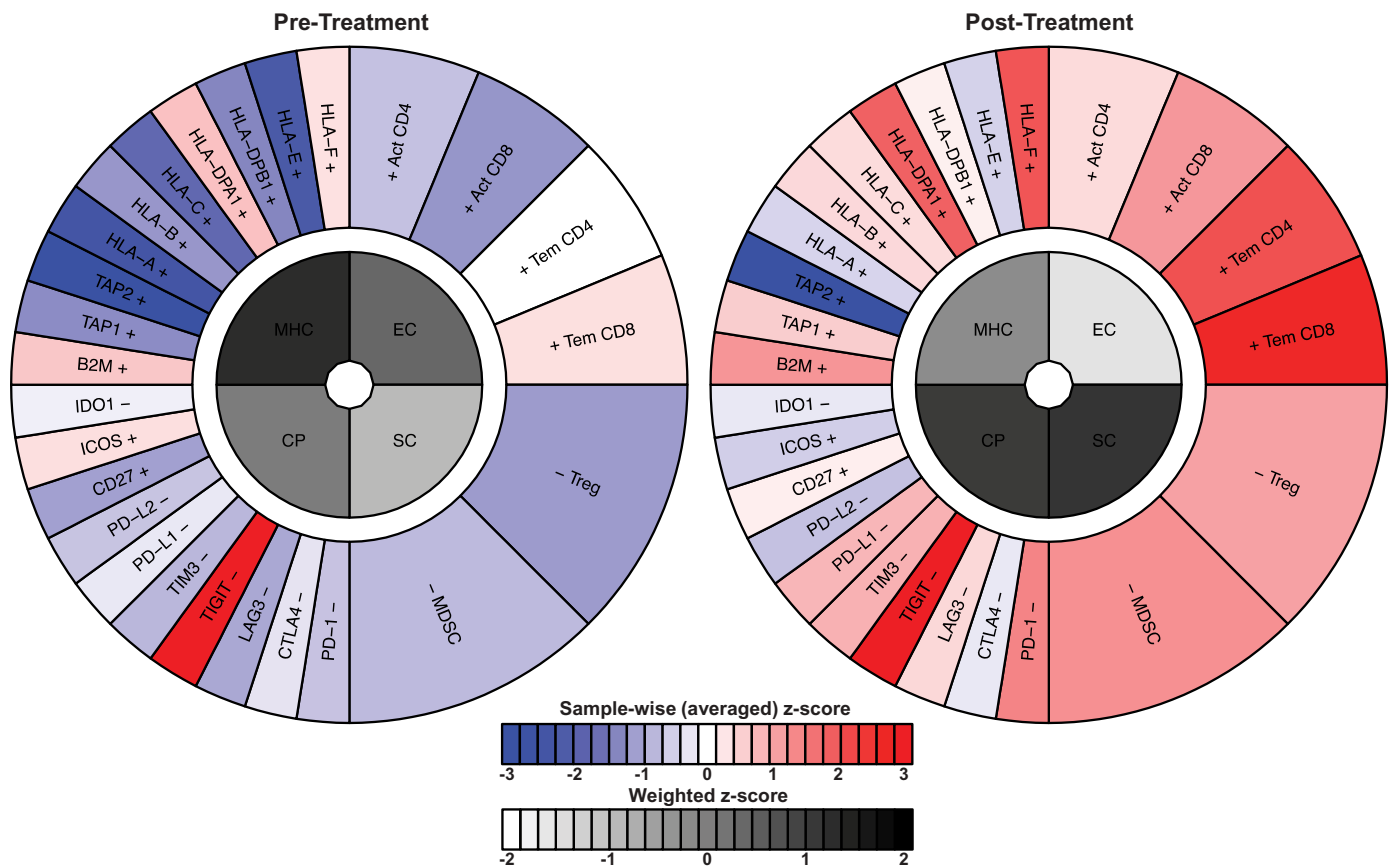
**Figure 6.** Modified immunophenoscore diagrams derived from Charoentong et al[21] for pre-treatment (top) and post-treatment (bottom) specimens. The gene or gene set comprising each point around the circle is labeled and grouped in corresponding quadrants. Red to blue color scale represent averaged z-score generated from 166 TCGA GBM samples. Grayscale represents weighted z-score associated with the composite score of each quadrant corresponding to the genes or gene sets within the quadrant. MHC = Major histocompatibility complex-associated and antigen presentation genes; CP = checkpoint molecules; EC = effector cells; SC = suppressor cells.

analysis demonstrated that all four modules were comparatively downregulated in the pre-treatment sample compared to the averaged TCGA GBM samples. In contrast, after treatment, all four modules exhibited increases over the averaged TCGA GBM z-scores, supporting the observation that both pro-inflammatory and immunoregulatory mechanisms were upregulated following treatment with radiation, chemotherapy, DCVax-L, and GBM.PVax.

## Discussion

Here, we describe the successful use of an immunogenomics pipeline to identify candidate neoantigens for incorporation into a personalized vaccine to treat GBM. Furthermore, the same immunogenomics pipeline was used to guide screening for neoantigen-specific T cell reactivity that may have been generated endogenously, as a result of prior treatment (surgery, radiation, chemotherapy or DCVax-L), or through epitope spreading. In total, we were able to detect reactivity to three HLA class I- and five HLA class II-restricted neoantigens from PBMC obtained post-treatment. Moreover, a similar pattern of reactivity was seen in post-treatment TIL, suggesting that systemically generated responses are capable of homing to and infiltrating CNS tumors. Lack of adequate pre-vaccination samples restricted our analysis

regarding the kinetics of these responses, but we were able to demonstrate an augmentation of neoantigen-specific T cell responses following vaccination. Regardless, these results support the rationale for targeting neoantigens even in lower mutational burden tumors like GBM, where the number of potentially immunogenic candidates is perhaps more limited than higher mutational tumors, such as melanoma. These results are further supported by the recent observation that an autologous tumor lysate-dendritic cell vaccine was shown to induce neoantigen-specific responses in ovarian cancer, another lower mutational burden tumor.[11,12]

These results combined with previously published reports[2,6,7] support the use of an immunogenomics pipeline to identify candidate neoantigens for personalized vaccines across multiple tumor types. It will now be necessary to determine the therapeutic value of neoantigen vaccine on improving clinical outcomes in patients, particularly in the setting of the recent phase 3 study showing no difference in overall survival with the addition of rindopepimut, a peptide vaccine targeting the neoantigen, EGFRvIII, to standard of care therapy for newly diagnosed GBM.[22] To this end, ongoing work by our group and others (NCT02149225, NCT02287428, NCT03223103, NCT03412877) is directed at evaluating the clinical efficacy of neoantigen-based vaccines in GBM.

Although the Rindopepimut vaccine targeting the junctional sequence created by the EGFRvIII variant also represented a neoantigen targeting approach, there are several differences between this approach and the cancer immunogenomics approach in this report. First, the EGFRvIII target is heterogeneously expressed, which could limit the efficacy of a vaccine directed at a single target due to therapy-induced immunoediting. However, by using a multi-valent vaccine platform such as the one described here, one can incorporate clonal neoantigens as well as neoantigens that may be expressed by different subclones to enhance the potential of targeting a greater proportion of tumor cells. Second, while rindopepimut efficiently generated robust EGFRvIII-specific humoral responses,[22] it has not been shown to induce a cytotoxic T cell response. Thus, a vaccine approach that can generate neoantigen-specific cell-mediated immune responses may be more effective. Third, patients were not selected for rindopepimut vaccine by MHC haplotype. Although predictions of neoantigen binding to HLA molecules are imperfect, the consideration of target affinity may increase the likelihood of effective T cell priming and target recognition in patients following vaccine treatment.

It is likely that combination immunotherapies will be necessary to increase therapeutic efficacy. Specifically, many personalized neoantigen vaccine approaches are combining tailored vaccines with immune modulating agents, such as checkpoint blockade therapy. Since neither vaccines nor immune checkpoint blockade therapy have been shown to improve survival of patients with GBM as monotherapies,[22-24] the combination of several complementary immune-based strategies may potentially be more effective. For example, the addition of a vaccine may improve checkpoint blockade therapy by inducing or increasing the number of tumor-specific T cells present within the tumor microenvironment.[8,17,18] Conversely, checkpoint blockade therapy may improve the effector function of vaccine-induced T cells once they home to the immunosuppressive tumor microenvironment.[25,26] Thus, while immunotherapies have yet to translate into improved survival for patients with GBM, a combinatorial immune-based approach may lead to better outcomes in the future.

It will also be important to determine the optimal methods of vaccination to stimulate the most robust and functional neoantigen-specific responses to the largest number of candidates per patient. For example, in this case, a heterologous prime-boost personalized vaccine approach of DCVax-L followed by synthetic long peptides was administered. Additional vaccine platforms – including nucleic acids and viral/bacterial vectors – warrant study. Moreover, identifying the ideal adjuvant including TLR agonists, immune checkpoint agonists/antagonists, or cytokines is an additional variable that has yet to be fully addressed.

Although we recognize the limitations from a single patient study, further consideration is needed with regard to monitoring the anti-tumor effects of vaccines in the CNS. Specifically, it is challenging to determine the efficacy of immune-based treatments in a tissue site, in this case, the CNS, in which it is more difficult to sample tissue iteratively to understand *in situ* immune activity. As a proxy for immune activity at the tumor site, we identified neoantigen-specific T cell responses in the blood, and we were able to culture neoantigen-specific TIL from the redo surgery sample. However, we did not observe a robust T cell infiltrate at the time of the patient's second surgery, a finding that was supported by our gene expression analysis. These findings raise the possibility that further study is needed to understand the kinetics of T cell homing to the CNS following vaccination. Additionally, these data underscore the influence of the large myeloid compartment within the GBM microenvironment. Further study is necessary to understand how to effectively enhance neoantigen-specific T cell activity, the effects of vaccines on the microenvironment, and how these parameters change with combination treatment.

The presence of pseudoprogression on the post-vaccination MRI represents another important consideration for vaccine trials in GBM as well as other novel immunotherapeutic strategies targeting CNS malignancies such as CAR T cells.[27] Radiographically assessing treatment response may be difficult as there are currently no criteria that can accurately and reliably delineate immune reactivity or inflammation from true tumor progression. This has begun to be addressed in the setting of immune checkpoint blockade therapy and brain metastases with the development of the Immunotherapy Response Assessment in Neuro-Oncology (iRANO).[28] However, in order to spare patients unnecessary surgical procedures or changes in otherwise effective therapies, novel imaging modalities or adjunct non-invasive monitoring assays will be needed.

Lastly, further work is needed to understand the emergence of resistant subclones post-treatment despite the presence of antigen-specific T cells. Neoantigenic and molecular profiling of the post-treatment tumor and microenvironment, respectively, may provide insight into potential immune evasion mechanisms. Specifically, the lack of expressed immunogenic neoantigens private to the resistant subclones suggests escape of active immunosurveillance. Conversely, while not observed in this case, it is plausible to postulate that treatment-induced changes from radiation and alkylating chemotherapies may lead to the development of new candidate neoantigens that could be targeted iteratively. Furthermore, the concomitant upregulation of immunoregulatory factors, such as inhibitory checkpoint molecules and suppressive immune cell subsets, supports the rationale for combining neoantigen-based vaccines with additional immunomodulatory strategies such as immune checkpoint blockade and microenvironment modulators[6,7] to augment the potency of these individual strategies.

In summary, the results presented herein provide proof-of-principle evidence supporting the feasibility of an immunogenomics-guided neoantigen discovery platform to design personalized vaccines in both CNS and lower mutational burden tumors.

## Materials and methods

Informed consent was signed prior to enrollment. All procedures and experiments were performed in accordance with the Declaration of Helsinki and an Institutional Review Board-

approved protocol at the Washington University School of Medicine. This study is NCT02510950 on clinicaltrials.gov.

### Whole exome DNA and RNA sequencing

Library construction, sequencing, and variant detection were performed as described.[29] Briefly, normal and tumor exome libraries were captured using the Nimblegen VCRome kit and cDNA was prepared with the TruSeq Stranded Total RNA kit. Each library was sequenced on an Illumina HiSeq2500. Somatic variants were detected using an ensemble approach incorporating statistical and heuristic filters. RNA-sequencing (RNA-seq) data were processed with Tophat v2.0.8 and Cufflinks v2.1.1 to generate gene expression values.[29]

### HLA class I and II neoantigen predictions, prioritization, and selection

Clinical HLA typing was performed. HLA alleles, annotated somatic variants, and FPKM-based variant expression values were used as pVAC-Seq inputs (www.pvactools.org),[16] which queries the IEDB algorithm collection to predict HLA class I neoantigen binding. Averaged binding affinities of NetMHCIIpan 3.2 and NetMHCII 2.3 were used for predicting HLA class II antigens. Candidate neoantigens for GBM.PVax were based on multiple factors including predicted HLA class I and/or II binding affinity, RNA-seq expression level, clonality, predicted peptide solubility, and targeted HLA allele diversification.

### Long peptide synthesis and GBM.PVax administration

Fifteen neoantigens were selected for synthetic long peptide production. Ultimately, eight peptides targeting seven candidate neoantigens were soluble and incorporated into GBM.PVax (Figure 1(b)). GMP grade peptides were produced by CS Bio (Menlo Park, CA). Three peptide pools containing 2–3 peptides/pool were dissolved in DMSO and diluted to 1 mg/peptide in D5W containing succinate. For vaccination, each peptide pool was co-administered subcutaneously with 1.5 mg poly-ICLC (Hiltonol; Oncovir, Washington, DC) into one of four rotating injection sites (right arm, left arm, right groin, left groin). Vaccinations were given on days 1, 3, 5, 8, 15, and 22 (±1 day) of cycle one and then on day 22 of every subsequent 28-day cycle (Figure 1(a)).

### Isolation of PBMC and Ex Vivo Expansion of TIL

Heparinized blood was collected by venipuncture prior to GBM. PVax initiation and by leukapheresis after GBM.PVax cycle 4. Peripheral blood mononuclear cells (PBMC) were isolated by Ficoll-Paque (GE Healthcare Life Sciences, Pittsburgh, PA) density gradient centrifugation and cryopreserved in 10% DMSO, 20% FBS, and culture media (RPMI-1640, L-glutamine, penicillin/streptomycin, β-mercaptoethanol, sodium bicarbonate, sodium pyruvate, 10% heat-inactivated FBS).

TIL were isolated by mincing the resected specimen into 1–2 mm chunks and incubating at 37°C in culture media with 2500 U/mL recombinant human IL-2 (EMED Medical Company, Maryland Heights, MO). Media was changed every 5–7 days. After 3 weeks, lymphocytes were harvested by Percoll (GE Healthcare Life Sciences) density gradient centrifugation and cryopreserved. Cells were stored in liquid nitrogen.

### IFN-γ ELISPOT assay

CD8$^+$ and CD4$^+$ cells were isolated from PBMC and TIL using sequential magnetic bead-based positive selection kits (STEMCELL Technologies, Vancouver, Canada). Approximately 100,000 double-negative autologous PBMC were incubated on pre-coated human IFN-γ ELISPOT plates (Cellular Technology, Ltd., Shaker Heights, OH) with 10 μM of indicated peptide (GenScript, Piscataway, NJ) plus ~400,000 CD8$^+$ or CD4$^+$ PBMC, or ~20,000 CD8$^+$ or CD4$^+$ TIL for 18–20 hours at 37°C. Plates were analyzed using the C.T.L. ImmunoSpot kit (Cellular Technology, Ltd., Shaker Heights, OH).

### Analysis of clonal evolution and transcriptome

Clonal evolution was analyzed as described previously.[29] Briefly, the SciClone algorithm was used to infer clonal hierarchy,[30] and clonEvol was used to reconstruct tumor phylogeny.[31] For gene set enrichment analysis, gene-specific expression levels from pre- and post-treatment specimens were z-score normalized across 166 TCGA-GBM patients as described previously.[21] Immunophenogram figures were generated using the publicly available R code on GitHub (https://github.com/mui-icbi/Immunophenogram).

### Statistical analysis

Intergroup differences in mean number of spots on ELISPOT were evaluated using a Student's $t$-test with $p < 0.05$ as statistically significant (GraphPad Prism, San Diego, CA).

## References

1. Schumacher TN, Schreiber RD. Neoantigens in cancer immunotherapy. Science. 2015;348:69–74. doi:10.1126/science.aaa4971.
2. Carreno BM, Magrini V, Becker-Hapak M, Kaabinejadian S, Hundal J, Petti AA, Ly A, Lie W-R, Hildebrand WH, Mardis ER, et al. Cancer immunotherapy. A dendritic cell vaccine increases the breadth and diversity of melanoma neoantigen-specific T cells. Science. 2015;348:803–808. doi:10.1126/science.aaa3828.
3. Gubin MM, Artyomov MN, Mardis ER, Schreiber RD. Tumor neoantigens: building a framework for personalized cancer immunotherapy. J Clin Invest. 2015;125:3413–3421. doi:10.1172/JCI80008.
4. Johanns TM, Bowman-Kirigin JA, Liu C, Dunn GP. Targeting neoantigens in glioblastoma: an overview of cancer

immunogenomics and translational implications. Neurosurgery. 2017;64:165–176. doi:10.1093/neuros/nyx321.

5. Johanns TM, Dunn GP. Applied cancer immunogenomics: leveraging neoantigen discovery in glioblastoma. Cancer J. 2017;23:125–130. doi:10.1097/PPO.0000000000000247.

6. Ott PA, Hu Z, Keskin DB, Shukla SA, Sun J, Bozym DJ, Zhang W, Luoma A, Giobbie-Hurder A, Peter L, et al. An immunogenic personal neoantigen vaccine for patients with melanoma. Nature. 2017;547:217–221. doi:10.1038/nature22991.

7. Sahin U, Derhovanessian E, Miller M, Bp K, Simon P, Lower M, Bukur V, Tadmor AD, Luxemburger U, Schrörs B, et al. Personalized RNA mutanome vaccines mobilize poly-specific therapeutic immunity against cancer. Nature. 2017;547:222–226. doi:10.1038/nature23003.

8. Gubin MM, Zhang X, Schuster H, Caron E, Ward JP, Noguchi T, Ivanova Y, Hundal J, Arthur CD, Krebber W-J, et al. Checkpoint blockade cancer immunotherapy targets tumour-specific mutant antigens. Nature. 2014;515:577–581. doi:10.1038/nature13988.

9. Yadav M, Jhunjhunwala S, Phung QT, Lupardus P, Tanguay J, Bumbaca S, Franci C, Cheung TK, Fritsche J, Weinschenk T, et al. Predicting immunogenic tumour mutations by combining mass spectrometry and exome sequencing. Nature. 2014;515:572–576. doi:10.1038/nature14001.

10. Johanns TM, Ward JP, Miller CA, Wilson C, Kobayashi DK, Bender D, Fu Y, Alexandrov A, Mardis ER, Artyomov MN, et al. Endogenous neoantigen-specific CD8 T cells identified in two glioblastoma models using a cancer immunogenomics approach. Cancer Immunol Res. 2016;4:1007–1015. doi:10.1158/2326-6066.CIR-16-0156.

11. Tanyi JL, Bobisse S, Ophir E, Tuyaerts S, Roberti A, Genolet R, Baumgartner P., Stevenson B.J., Iseli C., Dangaj D,.et al. Personalized cancer vaccine effectively mobilizes antitumor T cell immunity in ovarian cancer. Sci Transl Med. 2018;10 (436):eaao5931. doi:10.1126/scitranslmed.aao5931.

12. Bobisse S, Genolet R, Roberti A, Tanyi JL, Racle J, Stevenson BJ, Iseli C, Michel A, Le Bitoux M-A, Guillaume P, et al. Sensitive and frequent identification of high avidity neo-epitope specific CD8 (+) T cells in immunotherapy-naive ovarian cancer. Nat Commun. 2018;9:1092. doi:10.1038/s41467-018-03301-0.

13. Eckel-Passow JE, Lachance DH, Molinaro AM, Walsh KM, Decker PA, Sicotte H, Pekmezci M, Rice T, Kosel ML, Smirnov IV, et al. Glioma groups based on 1p/19q, IDH, and TERT promoter mutations in tumors. N Engl J Med. 2015;372:2499–2508. doi:10.1056/NEJMoa1407279.

14. Hegi ME, Diserens AC, Gorlia T, Hamou MF, de Tribolet N, Weller M, Kros JM, Hainfellner JA, Mason W, Mariani L, et al. MGMT gene silencing and benefit from temozolomide in glioblastoma. N Engl J Med. 2005;352:997–1003. doi:10.1056/NEJMoa043331.

15. Stupp R, Mason WP, van den Bent MJ, Weller M, Fisher B, Taphoorn MJ, Belanger K, Brandes AA, Marosi C, Bogdahn U, et al. Radiotherapy plus concomitant and adjuvant temozolomide for glioblastoma. N Engl J Med. 2005;352:987–996. doi:10.1056/NEJMoa043330.

16. Hundal J, Carreno BM, Petti AA, Linette GP, Griffith OL, Mardis ER, Griffith M. pVAC-Seq: A genome-guided in silico approach to identifying tumor neoantigens. Genome Med. 2016;8:11. doi:10.1186/s13073-016-0264-5.

17. Anagnostou V, Smith KN, Forde PM, Niknafs N, Bhattacharya R, White J, Zhang T, Adleff V, Phallen J, Wali N, et al. Evolution of neoantigen landscape during immune checkpoint blockade in non-small cell lung cancer. Cancer Discov. 2017;7:264–276. doi:10.1158/2159-8290.CD-16-0828.

18. George S, Miao D, Demetri GD, Adeegbe D, Rodig SJ, Shukla S, Lipschitz M, Amin-Mansour A, Raut CP, Carter SL, et al. Loss of PTEN is associated with resistance to anti-PD-1 checkpoint blockade therapy in metastatic uterine leiomyosarcoma. Immunity. 2017;46:197–204. doi:10.1016/j.immuni.2017.02.001.

19. Gabrusiewicz K, Rodriguez B, Wei J, Hashimoto Y, Healy LM, Maiti SN, Thomas G., Zhou S., Wang Q., Elakkad A, et al. Glioblastoma-infiltrated innate immune cells resemble M0 macrophage phenotype. JCI Insight. 2016;1(2):e85841. doi:10.1172/jci.insight.85841.

20. Antonios JP, Soto H, Everson RG, Moughon D, Orpilla JR, Shin NP, Sedighim S, Treger J, Odesa S, Tucker A, et al. Immunosuppressive tumor-infiltrating myeloid cells mediate adaptive immune resistance via a PD-1/PD-L1 mechanism in glioblastoma. Neuro Oncol. 2017;19:796–807. doi:10.1093/neuonc/now287.

21. Charoentong P, Finotello F, Angelova M, Mayer C, Efremova M, Rieder D, Hackl H, Trajanoski Z. Pan-cancer immunogenomic analyses reveal genotype-immunophenotype relationships and predictors of response to checkpoint blockade. Cell Rep. 2017;18:248–262. doi:10.1016/j.celrep.2016.12.019.

22. Weller M, Butowski N, Tran DD, Recht LD, Lim M, Hirte H, Ashby L, Mechtler L, Goldlust SA, Iwamoto F, et al. Rindopepimut with temozolomide for patients with newly diagnosed, EGFRvIII-expressing glioblastoma (ACT IV): a randomised, double-blind, international phase 3 trial. Lancet Oncol. 2017;18:1373–1385. doi:10.1016/S1470-2045(17)30517-X.

23. Liau LM, Ashkan K, Tran DD, Campian JL, Trusheim JE, Cobbs CS, Heth JA, Salacz M, Taylor S, D'Andre SD, et al. First results on survival from a large Phase 3 clinical trial of an autologous dendritic cell vaccine in newly diagnosed glioblastoma. J Transl Med. 2018;16:142. doi:10.1186/s12967-018-1507-6.

24. Omuro A, Vlahovic G, Lim M, Sahebjam S, Baehring J, Cloughesy T, Voloschin A, Ramkissoon SH, Ligon KL, Latek R, et al. Nivolumab with or without ipilimumab in patients with recurrent glioblastoma: results from exploratory phase I cohorts of CheckMate 143. Neuro Oncol. 2018;20:674–686. doi:10.1093/neuonc/nox208.

25. Lopes A, Vanvarenberg K, Kos S, Lucas S, Colau D, Van den Eynde B, Préat V, Vandermeulen G. Combination of immune checkpoint blockade with DNA cancer vaccine induces potent antitumor immunity against P815 mastocytoma. Sci Rep. 2018;8:15732. doi:10.1038/s41598-018-33933-7.

26. Kinkead HL, Hopkins A, Lutz E, Wu AA, Yarchoan M, Cruz K, Woolman S, Vithayathil T, Glickman LH, Ndubaku CO, et al. Combining STING-based neoantigen-targeted vaccine with checkpoint modulators enhances antitumor immunity in murine pancreatic cancer. JCI Insight. 2018;3(20):122857. doi:10.1172/jci.insight.122857.

27. O'Rourke DM, Nasrallah MP, Desai A, Melenhorst JJ, Mansfield K, Morrissette JJD, Martinez-Lage M, Brem S, Maloney E, Shen A, et al. A single dose of peripherally infused EGFRvIII-directed CAR T cells mediates antigen loss and induces adaptive resistance in patients with recurrent glioblastoma. Sci Transl Med. 2017;9(399):eaaa0984. doi:10.1126/scitranslmed.aaa0984.

28. Okada H, Weller M, Huang R, Finocchiaro G, Gilbert MR, Wick W, Ellingson BM, Hashimoto N, Pollack IF, Brandes AA, et al. Immunotherapy response assessment in neuro-oncology: a report of the RANO working group. Lancet Oncol 2015; 16: e534–e42. doi:10.1016/S1470-2045(15)00088-1.

29. Johanns TM, Miller CA, Dorward IG, Tsien C, Chang E, Perry A, Uppaluri R, Ferguson C, Schmidt RE, Dahiya S, et al. Immunogenomics of hypermutated glioblastoma: a patient with germline POLE deficiency treated with checkpoint blockade immunotherapy. Cancer Discov. 2016;6:1230–1236. doi:10.1158/2159-8290.CD-16-0575.

30. Miller CA, White BS, Dees ND, Griffith M, Welch JS, Griffith OL, Vij R, Tomasson MH, Graubert TA, Walter MJ, et al. SciClone: inferring clonal architecture and tracking the spatial and temporal patterns of tumor evolution. PLoS Comput Biol. 2014;10: e1003665. doi:10.1371/journal.pcbi.1003665.

31. Ding L, Tj L, De L, Ca M, Dc K, Js W, Ritchey JK, Young MA, Lamprecht T, McLellan MD, et al. Clonal evolution in relapsed acute myeloid leukaemia revealed by whole-genome sequencing. Nature. 2012;481:506–510. doi:10.1038/nature10738.